

# Coculture of adipose-derived mesenchymal stem cells/macrophages on decellularized placental sponge promotes differentiation into the osteogenic lineage

Citation for published version (APA):

Khosrowpour, Z., Hashemi, S. M., Mohammadi-Yeganeh, S., Moghtadaei, M., Brouki Milan, P., Moroni, L., Kundu, S. C., & Gholipourmalekabadi, M. (2023). Coculture of adipose-derived mesenchymal stem cells/macrophages on decellularized placental sponge promotes differentiation into the osteogenic lineage. *Artificial Organs*, 47(1), 47-61. <https://doi.org/10.1111/aor.14394>

## Document status and date:

Published: 01/01/2023

## DOI:

[10.1111/aor.14394](https://doi.org/10.1111/aor.14394)

## Document Version:

Publisher's PDF, also known as Version of record

## Document license:

Taverne

## Please check the document version of this publication:

- A submitted manuscript is the version of the article upon submission and before peer-review. There can be important differences between the submitted version and the official published version of record. People interested in the research are advised to contact the author for the final version of the publication, or visit the DOI to the publisher's website.
- The final author version and the galley proof are versions of the publication after peer review.
- The final published version features the final layout of the paper including the volume, issue and page numbers.

[Link to publication](#)

## General rights

Copyright and moral rights for the publications made accessible in the public portal are retained by the authors and/or other copyright owners and it is a condition of accessing publications that users recognise and abide by the legal requirements associated with these rights.

- Users may download and print one copy of any publication from the public portal for the purpose of private study or research.
- You may not further distribute the material or use it for any profit-making activity or commercial gain
- You may freely distribute the URL identifying the publication in the public portal.

If the publication is distributed under the terms of Article 25fa of the Dutch Copyright Act, indicated by the "Taverne" license above, please follow below link for the End User Agreement:

[www.umlib.nl/taverne-license](http://www.umlib.nl/taverne-license)

## Take down policy

If you believe that this document breaches copyright please contact us at:



[repository@maastrichtuniversity.nl](mailto:repository@maastrichtuniversity.nl)

providing details and we will investigate your claim.

Download date: 19 Mar. 2023

**MAIN TEXT**

# Coculture of adipose-derived mesenchymal stem cells/macrophages on decellularized placental sponge promotes differentiation into the osteogenic lineage

Zahra Khosrowpour<sup>1,2</sup> | Seyed Mahmoud Hashemi<sup>3</sup>  |  
 Samira Mohammadi-Yeganeh<sup>4,5</sup> | Mehdi Moghtadaei<sup>2,6</sup> | Peiman Brouki Milan<sup>1,2</sup> |  
 Lorenzo Moroni<sup>7</sup> | Subhas C. Kundu<sup>8</sup> | Mazaher Gholipourmalekabadi<sup>1,9,2</sup> 

<sup>1</sup>Cellular and Molecular Research Centre, Iran University of Medical Sciences, Tehran, Iran

<sup>2</sup>Department of Tissue Engineering & Regenerative Medicine, Faculty of Advanced Technologies in Medicine, Iran University of Medical Sciences, Tehran, Iran

<sup>3</sup>Department of Immunology, School of Medicine, Shahid Beheshti University of Medical Sciences, Tehran, Iran

<sup>4</sup>Medical Nanotechnology and Tissue Engineering Research Center, Shahid Beheshti University of Medical Sciences, Tehran, Iran

<sup>5</sup>Department of Medical Biotechnology, School of Advanced Technologies in Medicine, Shahid Beheshti University of Medical Sciences, Tehran, Iran

<sup>6</sup>Orthopaedic Department, Hazrat-Rasul Hospital, Faculty of Medicine, Iran University of Medical Sciences, Tehran, Iran

<sup>7</sup>Complex Tissue Regeneration Department, Maastricht University, MERLN Institute for Technology-Inspired Regenerative Medicine, Maastricht, The Netherlands

<sup>8</sup>3Bs Research Group, I3Bs - Research Institute on Biomaterials, Biodegradable and Biomimetics, Headquarters of the European Institute of Excellence on Tissue Engineering and Regenerative Medicine, University of Minho, Guimaraes, Portugal

<sup>9</sup>Department of Medical Biotechnology, Faculty of Allied Medicine, Iran University of Medical Sciences, Tehran, Iran

**Correspondence**

Seyed Mahmoud Hashemi, Department of Immunology, Shahid Beheshti University of Medical Sciences, Arabi Ave, Daneshjoo Blvd, Velenjak, Tehran, Iran.

Email: [smmhashemi@sbmu.ac.ir](mailto:smmhashemi@sbmu.ac.ir)

Mazaher Gholipourmalekabadi, Department of Medical Biotechnology, Iran University of Medical Sciences, Hemmat Highway, Tehran 144961-4535, Iran.

Email: [mazaher.gholipour@gmail.com](mailto:mazaher.gholipour@gmail.com); [mazaher.gholipour@iums.ac.ir](mailto:mazaher.gholipour@iums.ac.ir)

**Funding information**

Iran University of Medical Sciences, Grant/Award Number: 16775; Shahid Beheshti University of Medical Sciences

**Abstract**

**Background:** Several factors like three-dimensional microstructure, growth factors, cytokines, cell–cell communication, and coculture with functional cells can affect the stem cells behavior and differentiation. The purpose of this study was to investigate the potential of decellularized placental sponge as adipose-derived mesenchymal stem cells (AD-MSCs) and macrophage coculture systems, and guiding the osteogenic differentiation of stem cells.

**Methods:** The decellularized placental sponge (DPS) was fabricated, and its mechanical characteristics were evaluated using degradation assay, swelling rate, and pore size determination. Its structure was also investigated using hematoxylin and eosin staining and scanning electron microscopy. Mouse peritoneal macrophages and AD-MSCs were isolated and characterized. The differentiation potential of AD-MSCs co-cultured with macrophages was evaluated by RT-qPCR of osteogenic genes on the surface of DPS. The in vivo biocompatibility of DPS was determined by subcutaneous implantation of scaffold and histological evaluations of the implanted site.



**Results:** The DPS had 67% porosity with an average pore size of 238  $\mu\text{m}$ . The in vitro degradation assay showed around 25% weight loss during 30 days in PBS. The swelling rate was around 50% during 72 h. The coculture of AD-MSCs/macrophages on the DPS showed a significant upregulation of four differentiation osteogenic lineage genes in AD-MSCs on days 14 and 21 and a significantly higher mineralization rate than the groups without DPS. Subcutaneous implantation of DPS showed in vivo biocompatibility of scaffold during 28 days follow-up.

**Conclusions:** Our findings suggest the decellularized placental sponge as an excellent bone substitute providing a naturally derived matrix substrate with biostructure close to the natural bone that guided differentiation of stem cells toward bone cells and a promising coculture substrate for crosstalk of macrophage and mesenchymal stem cells in vitro.

#### KEYWORDS

bone tissue engineering, coculture, immunomodulation, macrophage, mesenchymal stem cells

## 1 | INTRODUCTION

Bone defects are the most common injuries resulting from trauma, tissue resection due to cancer, and congenital anomalies.<sup>1,2</sup> When the loss or damage is significant, a fundamental goal in medical advances is to develop methods to improve bone repair, using biomaterial scaffolds that can deliver cells to the defective site.<sup>3</sup> Bone repair includes proinflammation and regeneration stages.<sup>4</sup>

Mesenchymal stem cells (MSCs) are the progenitor cells with self-renewal capability that can differentiate into various lineages of mesodermal tissues, such as bone and cartilage.<sup>5</sup> Because of their immunomodulatory properties, they are attractive targets in cell therapy and regenerative medicine. Macrophages (MQ) present at all stages of fracture repair are one of the specific immune cells responsible for modulating the repair.<sup>6,7</sup> Macrophages have a critical role in regenerative medicine, and their absence in the place of injury can delay bone repair.<sup>8,9</sup> Some studies confirmed that local injection of macrophage colony-stimulating factor at the fracture site significantly enhanced the number of macrophages and subsequently improved bone formation.<sup>10</sup> In addition, the other studies showed that depletion of macrophages in MAFIA mice resulted in a reduction in bone formation.<sup>11</sup> Depending on received signals, macrophages can mainly be polarized into either a proinflammatory (M1) or anti-inflammatory (M2) phenotype.<sup>12</sup>

The M2 macrophages secrete anti-inflammatory cytokines, whereas M1 macrophages secrete proinflammatory cytokines. In the cite of injury, the M1 macrophages are the first dominant immune cell population that contributed to phagocytosis. Later on, they replaced the M2

macrophages, which contributed to regeneration due to secreting anti-inflammatory and growth factors. M1 macrophages secrete chemokines (CCL2, CXCL8, and SDF-1) that control progenitor cell homing and promote the recruitment, proliferation, and differentiation of progenitor cells.<sup>2</sup> MSCs secretions prompt the polarization of macrophages from M1 to M2 phenotype both in vitro and in vivo.<sup>13</sup> M2 macrophages can improve bone formation by inducing osteogenic differentiation of adipose tissue MSCs and secretion of oncostatin M (OSM).<sup>14</sup> To date, little research has so far focused on the macrophage-MSC interaction to improve bone formation. Nevertheless, the healing potential of these cells during the bone healing process makes them a promising treatment option to enhance bone healing.<sup>15</sup>

Coculture of MSCs/MQ suppressed the secretion of proinflammatory cytokines (TNF- $\alpha$ , IL-1 $\beta$ , and IL-6) from macrophages and induced the production of anti-inflammatory cytokines like IL-10.<sup>16</sup> It was also demonstrated that coculture of MSCs/human peripheral blood monocytes induced an anti-inflammatory phenotype in macrophages.<sup>17</sup> Based on the macrophage-MSC cross talk, there are two strategies for supporting bone formation: first, regulating the macrophages at the injury site; and second, modulating the polarization of local macrophages. Therefore, MSCs and macrophages can be used as treatment options to enhance fracture healing in bone regeneration studies. The cells show different behavior and function in 2D and 3D culture system. As a naturally derived matrix culture system, tissue engineering scaffolds are constructed and developed to provide biomechanical, structural, and biological properties similar to natural tissues and promote stem cell differentiation



and tissue regeneration both in vitro and in vivo.<sup>18,19</sup> For osteogenic differentiation, scaffolds should mimic the bone structure and morphology to provide a platform for cell transplantation and interaction and facilitate new bone formation.<sup>20</sup> Extracellular matrix (ECM) derived from the decellularization of the placenta has shown promising results in tissue engineering and regeneration.<sup>21</sup> Anti-inflammatory, anti-scarring, antibacterial, angiogenic, and biocompatibility properties of the placenta, and the ability to regulate cellular activity make it an excellent choice for using as a universal biologic scaffold for biomedical applications.<sup>21</sup> A healthy placenta is available universally with fewer ethical restrictions and greater availability as medical waste.<sup>22</sup> The placenta is dedicated to vascular networks for exchanging venous blood, sufficient space for transplanted cells, and ECM containing beneficial factors associated with vascular, mesenchymal, or other cell types. It has rich ECM content.<sup>23</sup> Promising results have also been reported using decellularized human placenta xenografts in animal models for tissue regeneration.<sup>24–26</sup> In the current study, we hypothesized that decellularized placental sponges (DPS) could provide an excellent naturally derived matrix platform and composition biomimicking the natural bone tissue for coculture of macrophages and AD-MSCs and promote the AD-MSCs differentiation toward the osteogenic lineages.

## 2 | MATERIALS AND METHODS

### 2.1 | Placental tissue collection

Human placentas were harvested from the caesarean section deliveries of the consenting mothers, according to the procedures approved by the Ethics Committee at Iran University of Medical Sciences under approval ID of “IR.IUMS.REC.1398.1382.”

### 2.2 | Preparation of decellularized placental sponge (DPS)

The decellularized placental sponge (DPS) was fabricated by a protocol described by Asgari et al.<sup>27</sup> Briefly, the placental tissue was dissected into random small pieces, washed with distilled water, then homogenized for 10 min using a blender. The homogenized samples were treated with 0.5% sodium dodecyl sulfate (SDS) and 0.5% Triton™ X-100 (both from Sigma Aldrich, St. Louis, MO, USA) and put on a shaker for 30 min. Then they were washed with phosphate-buffered saline (PBS) (Sigma Aldrich, St. Louis, MO, USA) and centrifuged at

2000 rpm for 10 min. This stage was repeated for 10 days and each day 20 times. The decellularized placental was mixed with distilled water in the proportion of 1:2 (vol/vol), then poured into 60 mm petri dishes, and frozen at  $-80^{\circ}\text{C}$  overnight. Then they were freeze-dried (Alpha 1–2 LD plus, Christ, Germany) for 24 h. The freeze-dried scaffolds were kept at  $-20^{\circ}\text{C}$ .

### 2.3 | Decellularized placental sponge characterization (DPS)

#### 2.3.1 | H&E staining

The DPS was fixed in 10% (vol/vol) neutral buffered formalin (NBF) for 5 days, then dehydrated through a graded ethanol series (30, 50, 70, 96, and 100%). After embedding in paraffin blocks, the samples were cut into 5-micron thick serial sections by a microtome (Thermo Fisher Scientific, Waltham, Massachusetts, USA). The H&E staining was used to confirm the successful removal of the cells.

#### 2.3.2 | Scanning electron microscope (SEM)

The freeze-dried DPS was sputter-coated with gold and then viewed under a scanning electron microscope (SEM, AIS2100; Seron Technology, Gyeonggi-do, South Korea) at a voltage of 15 kV.

#### 2.3.3 | Mechanical property

The DPS's mechanical behavior (compression test) was determined by a Universal Testing Machine (SANTAM-STM20, Tehran, Iran) with a crosshead loading rate of  $0.5\text{ mm}\cdot\text{min}^{-1}$  and a 10 kg load cell. The DPS was 11 mm in height and 12 mm in diameter.

#### 2.3.4 | Degradation assays

For evaluation of the in vitro degradation rate of the DPS, the samples ( $n = 3$ ) were weighted ( $W_0$ ), then immersed in 5 ml of PBS (pH 7.4) and incubated at  $37^{\circ}\text{C}$  for 3, 7, 10, 14, 21, and 30 consecutive days. After each time point, the samples were gently washed with distilled water, freeze-dried for 24 h, and then weighed ( $W_d$ ). The degradation rate (percent mass lost) was calculated by the following Equation (1):

$$\text{Degradation (\%)}: (W_0 - W_d) / W_0 \times 100 \quad (1)$$



### 2.3.5 | Swelling rate and porosity

The swelling rate of the DPS was measured by the gravimetric method.<sup>28</sup> The DPS samples ( $n = 3$ ) were weighted ( $W_0$ ) and immersed in PBS for 24 h at 37°C. The samples were weighed ( $W_s$ ) after removing the excess PBS by filter paper. The swelling ratio (%) was calculated by the following Equation (2):

$$\text{Swelling ratio (\%)}: (W_s - W_0) / W_0 \times 100 \quad (2)$$

The porosity of the DPS was measured by the ethanol displacement method.<sup>29</sup> In brief, 3 samples were weighed ( $W_d$ ) and placed in 5 ml of ethanol at 37°C for 30 min. The samples were removed from the ethanol and weighed ( $W_l$ ), then the extra water of samples was extracted using filter paper and weighed again ( $W_w$ ). The porosity (%) was measured using the following Equation (3):

$$\text{Porosity (\%)}: (W_w - W_d) / (W_w - W_l) \times 100 \quad (3)$$

### 2.3.6 | Pore size

The average diameter of pore size in the DPS was analyzed from eight random pores of scanning electron microscope (SEM) micrographs by ImageJ software (National Institute of Health, USA).

## 2.4 | DPS-cells interaction

The cell viability, cell attachment, and penetration of the cells into the DPS were determined using MTT assay, SEM, and hematoxylin and eosin staining, respectively.

### 2.4.1 | Cells isolation and characterizations

Male BALB/c mice at 5–7 weeks of age were used for AD-MSCs and macrophages isolation. Mice were bought from Pasture Institute, Tehran, Iran. They were housed under a standard condition according to the Guidelines for Care and Use of Laboratory Animals provided by Shahid Beheshti University of Medical Sciences, Tehran, Iran, with ethical approval ID of “IR.SBMU.MSP.REC.1399.777.”

#### *AD-MSCs isolation and characterization*

Mouse AD-MSCs were isolated from abdominal fat tissues of BALB/c mice.<sup>30</sup> Briefly, the adipose tissues were separated, washed with PBS, and digested with 0.075% type I collagenase (Sigma-Aldrich) in Dulbecco's Modified Eagle Medium (DMEM) at 37°C for 20 min. Digested fat tissues

were homogenized by pipetting and centrifuged at 500 g for 10 min. Then, the pellet was cultured in DMEM containing 10% fetal bovine serum (FBS) supplemented with penicillin, and streptomycin (all reagents were purchased from Invitrogen), incubated under a humidified air and 5% CO<sub>2</sub> atmosphere at 37°C. The AD-MSCs have reached 65%–70% confluence within 2 weeks.

For characterization of the isolated AD-MSCs, the cells at the third passage were suspended in a 10<sup>6</sup> cells/ml suspension in PBS contained with 0.05% tween-20 (TTBS). 100 μl of the suspension were stained with antibodies against CD105, CD73, CD11b, CD45, CD90, and CD44 of AD-MSCs (all were purchased from eBioscience). Then, they were measured by a FACSCalibur flow cytometer (BD Biosciences, USA) and Cyflogic software (CyFlo Ltd., Finland). The differentiation capacity of the isolated AD-MSCs was evaluated using Oil Red O (ORO) and Alizarin Red (AR) staining. For osteogenic differentiation, AD-MSCs were cultured in DMEM supplemented with 50 mg/ml ascorbic acid biphosphate (Sigma-Aldrich, USA), 10 mM beta-glycerophosphate (Merck, UK), and 100 nM dexamethasone (Sigma-Aldrich) for 21 days. For adipocyte differentiation, AD-MSCs were cultured in DMEM in the presence of 0.5 mM 3-isobutyl-1-methylxanthine (Sigma-Aldrich), 250 nM dexamethasone (Sigma-Aldrich), 5 mM insulin (Sigma-Aldrich), and 100 mM indomethacin (Sigma-Aldrich) for 21 days.

#### *Peritoneal macrophage isolation and characterization*

The macrophages were isolated from the peritoneal cavity of BALB/c mice by a published protocol.<sup>30</sup> 1 ml of 4% (w/v) Brewer's thioglycollate medium was injected into the peritoneal cavity of each BALB/c mouse. After 4 days, the macrophages were isolated by intraperitoneal injection of 10 ml cold DMEM medium. The harvested cells were centrifuged, and the cell pellets were cultured in adherent petri dishes. The isolated macrophages were diluted to 10<sup>6</sup> cells/ml in DMEM and phenotypically analyzed for the expression of CD11b and CD14 markers on their surface using a FACSCalibur flow cytometer and Cyflogic software, as described above. All antibodies were purchased from eBioscience (San Diego, CA).

### 2.4.2 | In vitro cyto-biocompatibility assay

In vitro cyto-biocompatibility of the DPS for AD-MSCs was analyzed using MTT assay, cell attachment, and H&E staining. 4 × 10<sup>4</sup> cells/ml AD-MSCs were cultured on DPS in DMEM supplemented with 10% FBS, 100 U/ml penicillin–streptomycin (pen/strep) (all from Gibco, Carlsbad, CA, USA), then incubated at 37°C for different time intervals, depending to the assays.



### Cell viability assay

The viability of the AD-MSCs on the DPS was determined by MTT assay.<sup>31</sup> In brief, after 3 and 7 days of the AD-MSCs growth on the DPS, the cell/scaffold constructs were washed with PBS, then treated with 10% (vol/vol) tetrazolium salt (MTT (3-[4,5-dimethylthiazol-2-yl]-2,5-diphenyltetrazolium bromide, Sigma Aldrich, St. Louis, MO, USA) in supplemented DMEM and incubated for 4 h at 37°C. The formazan crystals of living cells were dissolved with dimethyl sulfoxide (DMSO, Sigma Aldrich, St. Louis, MO, USA). The optical density of the purple color produced after the dissolution of formazan crystals was calculated by an ELISA microplate-reader (DYNEX, USA) at 570 nm. The viability of the cells in 48 well cell culture plates was a positive control (100% cell viability), and fresh cell culture media was considered the negative control (ODnc). The cell viability was computed using the following formula (4);

$$\text{Cell viability (\%)} = \frac{\text{OD of experiments} - \text{Average OD of negative controls}}{\text{Average OD of positive control}} \times 100 \quad (4)$$

### Cell attachment under SEM

On day 7 of the AD-MSCs growth on DPS, the cell/scaffold was gently washed with PBS, then fixed with 2.5% glutaraldehyde for 2 h, dehydrated in a graded ethanol series, and finally dried under vacuum. For taking SEM micrographs from the cell/scaffold, they were sputter-coated with gold and then observed under SEM (AIS2100; Seron Technology, South Korea).

### H&E staining

After 7 days of AD-MSCs growth on the DPS, the cell/scaffold construct was fixed with 10% (vol/vol) NBF; after H&E staining, it was observed under the light microscope (Olympus Corporation, Shinjuku, Tokyo, Japan), as described above.

## 2.4.3 | Macrophage/AD-MSCs coculture and bone lineage differentiation on DPS

### Coculture of macrophages/AD-MSCs on DPS

The DPS was used as a naturally derived matrix for the coculture of AD-MSCs and macrophages to determine its potential as a coculture system and bone lineage differentiation. For this purpose,  $5 \times 10^4$  AD-MSCs and  $5 \times 10^5$  macrophages (1:10 ratio) were cocultured on the DPS in different experimental groups of (i) Coculture of AD-MSCs/macrophages in 24-well plates; (ii) AD-MSCs in 24-well plates; (iii) Coculture of AD-MSC/macrophages on DPS, and (iv) AD-MSCs culture on DPS. The cells/DPS constructs were subjected to H&E staining and SEM.

For osteogenic differentiation of the AD-MSCs, the cells were cultured in DMEM supplemented with ten mM beta-glycerophosphate (Merck, UK), 50 mg/ml ascorbic acid biphosphate (Sigma–Aldrich, USA), and 100 nM dexamethasone (Sigma–Aldrich) for 14 and 21 days at 37°C. The osteogenic differentiation was assessed with real-time PCR and alizarin red (AR) staining.

### H&E staining

After 14 days of cultures on the DPS, the cell/scaffolds constructs were fixed and stained as described above.

### Phase-contrast microscopy

The effects of DPS on the morphologic shape of the cells (macrophages, AD-MSCs, and AD-MSCs/macrophages coculture), the cells were cultured in cell culture plates. The cells in groups III and IV were exposed to DPS. After

14 days, they were observed under the phase-contrast microscope (Olympus Corporation, Shinjuku, Tokyo, Japan).

### Cell attachment under SEM

The morphology of the cells after 14 days of growth on DPS, the cells/scaffold constructs were prepared for observation under SEM as described above.

### Alizarin red (AR) staining

After 21 days of induction with osteogenic factors, the groups were fixed with 4% paraformaldehyde in PBS for 20 min and then incubated with Alizarin Red S (2% solution, pH 4.1–4.3) for 10 min, then washed with PBS four times. Four random fields were captured using an inverted microscope and analyzed using ImageJ (National Institute of Health, USA).

### Real-time PCR

Total RNA from all the experimental groups was extracted by RNX-Plus (SinaClone BioScience, Tehran, Iran) at day 14 and 21 osteogenic differentiation induction.<sup>32</sup> The RNA samples were converted into cDNA by SinaClone BioScience Kit (SinaClone BioScience, Tehran, Iran). The gene expression of alkaline phosphatase (ALP), runt-related transcription factor 2 (Runx2), osteocalcin (OCN), osteopontin (OPN) was performed by an SYBR® Green Real-time PCR Master Mix (SMOBIO Technology, Hsinchu, Taiwan) and data were presented as  $2^{-\Delta\Delta ct}$ . The primers used in this study are own designed and listed in Table 1.

## 2.5 | In vivo biocompatibility

For evaluation of in vivo biocompatibility and angiogenic property, DPS scaffolds were implanted subcutaneously on the back of NMRI mice. The surgical procedure was

TABLE 1 Sequence of primers used in real-time RT-PCR gene

Gene name	Sequence
1 ALP	F: 5'-GGTAGATTACGCTCACAACA-3' R: 5'-CAGGCACAGTGGTCAA-3'
2 Runx2	F: 5'-AATGCCTCCGCTGTTA-3' R: 5'-TCTGTCTGTGCCCTTCTT-3'
3 OCN	F: 5'-ACCTCACAGATGCCAA-3' R: 5'-ACTACCTTATTGCCCTCC-3'
4 B2M	F: 5'-GCTATCCAGAAAACCCCTC-3' R: 5'-CCC GTTCTTCAGCATTG-3'
5 OPN	F: 5'-AACCAGCCAAGGACTAACT-3' R: 5'-CTTCAGAGGACACAGCAT-3'

carried out by a published protocol.<sup>33</sup> In brief, NMRI male mice ( $n = 3$ , 6–8 weeks, with an average weight of about 30 g) were purchased from the Pasture Institute (Tehran, Iran) and kept under a standard condition in the Animal Science Department. The animals were anesthetized by the intraperitoneal administration of ketamine (0.1 mg/kg, Anesketin, Heusden–Zolder, Belgium) and xylazine (0.01 mg/kg, Heusden–Zolder, Belgium). After back shaving, DPS scaffolds were implanted subcutaneously and then stitched. The site of implantation was harvested at days 7 and 28, fixed with 10% neutral buffered formalin, stained with H&E and observed under the light microscope (Olympus Corporation, Shinjuku, Tokyo, Japan).

## 2.6 | Statistical analysis

All data are expressed as means  $\pm$  standard deviation (SD). The significance level was calculated using the one-way

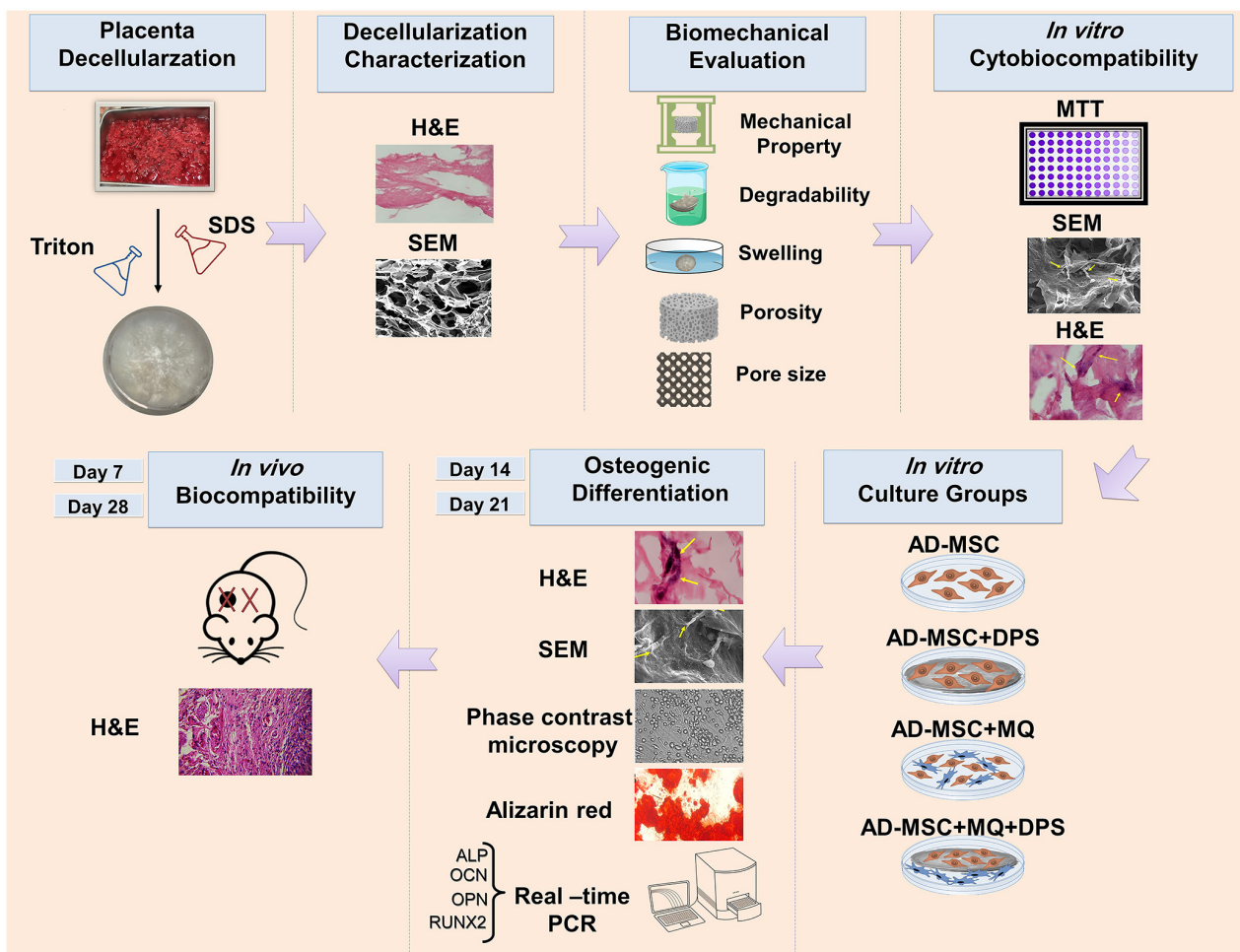
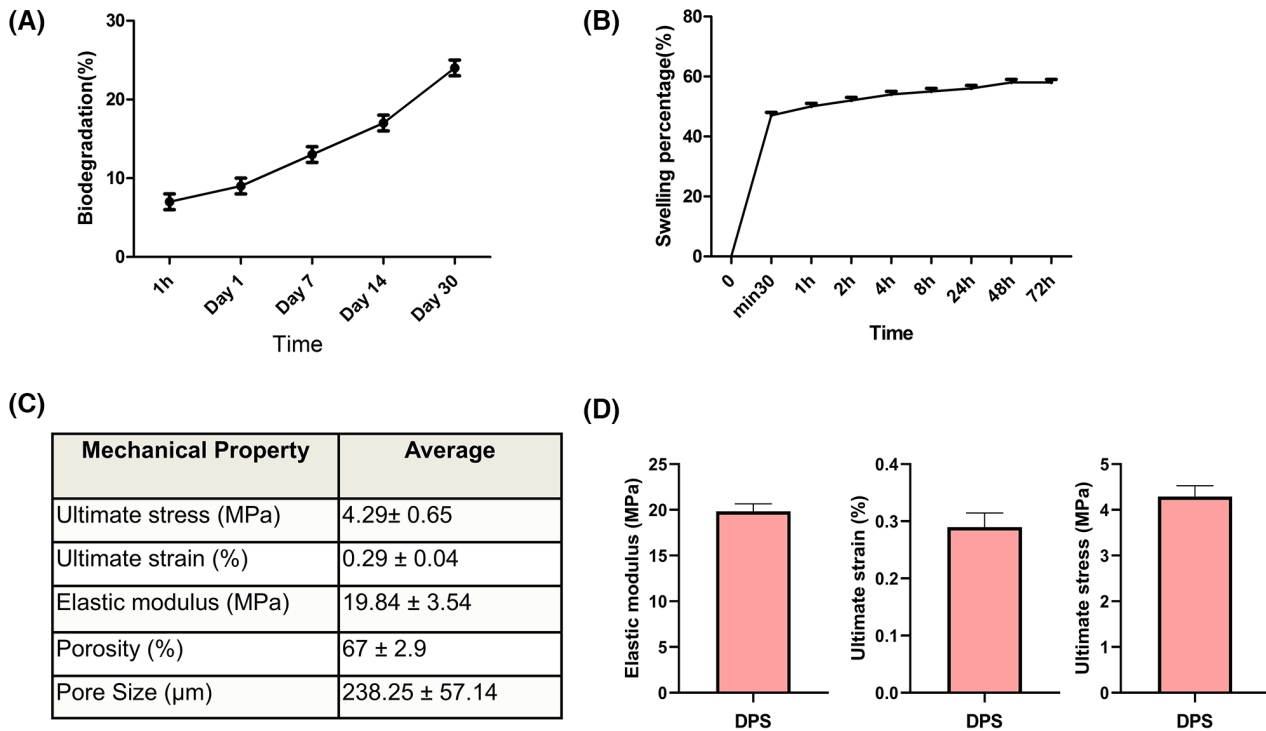
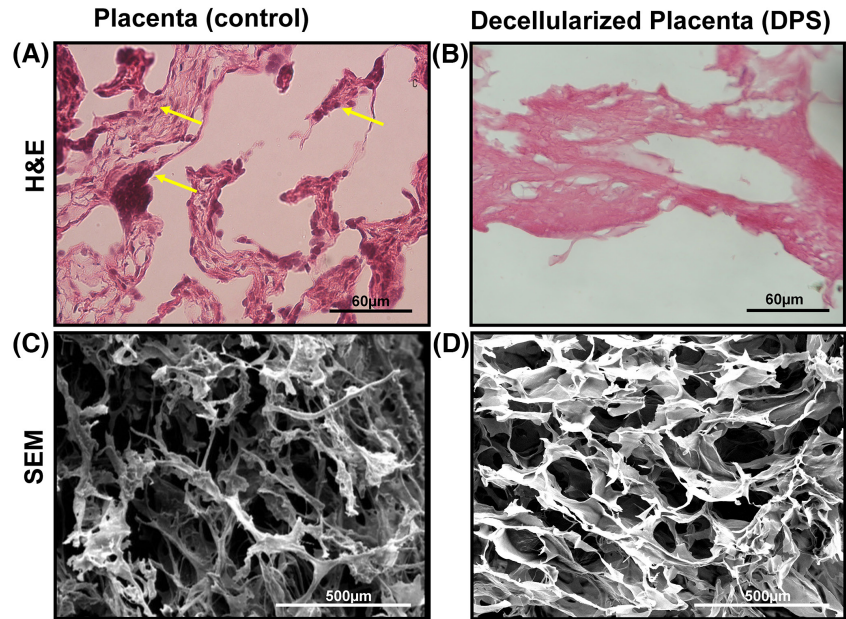


FIGURE 1 Summary of the current designed study plan. In this study the DPS was fabricated and evaluated as an excellent coculture system for AD-MSCs and macrophages for bone differentiation.

**FIGURE 2** H&E staining of (A) the placenta before (control) and (B) after decellularization processes. Yellow arrows show cell nuclei stained with hematoxylin in the control group. SEM micrographs of (C) the placenta before (control) and (D) after decellularization processes.



**FIGURE 3** (A) The in vitro degradation assay of DPS ( $n = 3$ ). (B) the swelling percentage of DPS during 72 h. (C) the mechanical property of DPS. (D) Graph of DPS mechanical property.

variance (ANOVA) analysis. Statistically, a significant difference was defined as the  $p$ -value  $< 0.05$ .

### 3 | RESULTS

The brief schematic of the study design is illustrated in Figure 1.

#### 3.1 | Placenta characterizations

##### 3.1.1 | H&E staining

The H&E stained sections of the placental tissues before (control) and after decellularization processes are presented in Figure 2A,B, respectively. The successful removal of the cells was confirmed in the DPS by histological observations.



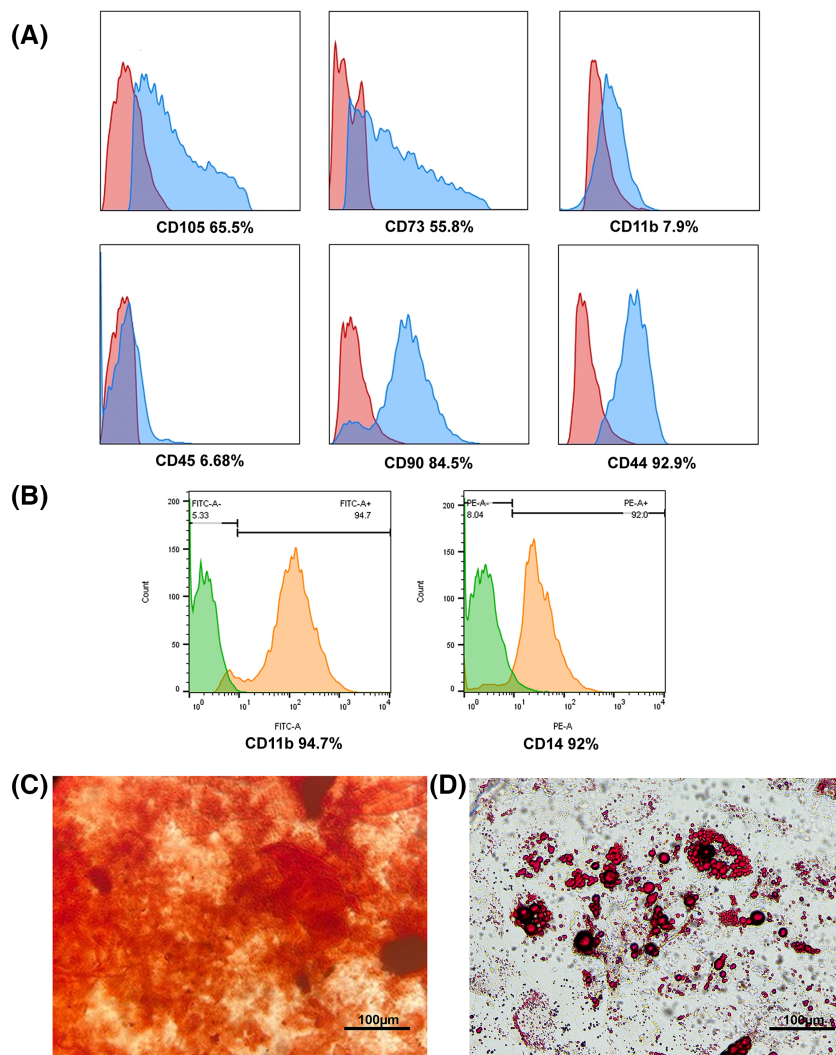


**FIGURE 4** Characterization of AD-MSCs and macrophages. (A) Flow cytometric analysis of the expression of AD-MSCs surface markers isolated from BALB/c strain. (B) Flow cytometric analysis of the expression of macrophages surface markers isolated from BALB/c strain. (C) Phase-contrast microscopy of alizarin red S staining for calcium mineralization of differentiated AD-MSCs to osteocyte, and (D) adipocytes by oil red O staining for lipid vacuoles.

### 3.1.2 | Scanning electron microscope (SEM)

Microstructures of the placental sponges before and after decellularization under SEM are presented in [Figure 2C,D](#). The DPS showed a porous microstructure with a high degree of interconnectivity. At the same time, the control scaffold had non-continuous pore channels with irregular microstructures.

### 3.1.3 | Degradability assays

The degradation results of the samples in PBS during 30 days are revealed in [Figure 3A](#). The degradation rate of the DPS at 1 h, 1 day, 7 days, 14 days, and 30 days was 6%, 10%, 14%, 19%, and 25%, respectively.

### 3.1.4 | Swelling rate and porosity (%)

Water uptake of the DPS showed a rapid increase (24%) during the first 30 min, then a slight increase during 72 h.

The swelling ratio of DPS increased from the average of 47% to 58% during 30 min to 72 h ([Figure 3B](#)). The DPS had a highly porous microstructure with inter-connective networks. The average porosity of the DPS was  $67 \pm 2.9\%$  ([Figure 3C](#)), which is sufficient for cell infiltration and the diffusion of oxygen and nutrients.<sup>29</sup>

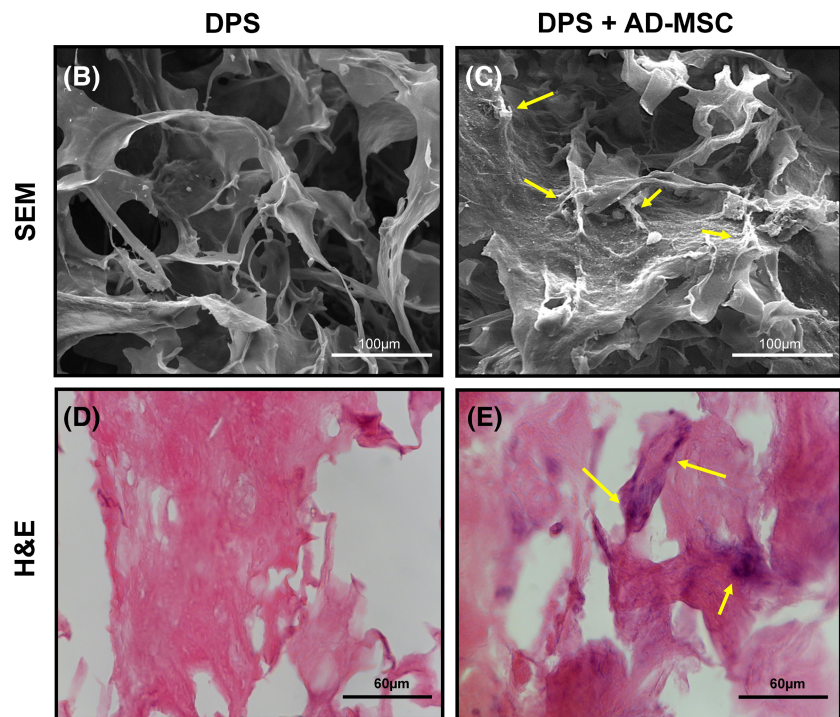
### 3.1.5 | Mean pore size (µm)

SEM micrographs were used for the assessment of the average pore size of the DPS. The mean pore size of DPS was  $238.25 \pm 57.14$  (µm) ([Figure 3C](#)).

### 3.1.6 | Mechanical property

DPS's ultimate stress and strain were  $4.29 \pm 0.65$  (MPa) and  $0.29 \pm 0.04\%$ , respectively. Also, the elastic modulus of DPS was  $19.84 \pm 3.54$  (MPa) ([Figure 3C,D](#)). The mechanical testing results suggest that the DPS has favorable mechanical characteristics as a bone substitute.

**FIGURE 5** (A) The MTT assay of the cells cultured on DPS at days 3 and 7. (B) SEM micrographs of the DPS without cells (control) and (C) AD-MSCs (yellow arrows) cultured on the DPS. (D) H&E staining of the DPS without cells (control) and (E) the DPS cultured with AD-MSCs. Yellow arrows show the cells penetrated and grown within the pores of DPS.



## 3.2 | DPS-cells interactions

### 3.2.1 | Characterization of the isolated cells

At passage 3, flow cytometry was used to demonstrate the expressions of cell surface markers containing CD73, CD105, CD11b, CD45, CD90, and CD44 for AD-MSCs and CD45 and CD11b for peritoneal macrophages. AD-MSCs showed a very low expression of CD11b and CD45 at mean percentages of 6.68% and 7.9%, respectively, and high expression of CD105, CD44, CD73, and CD90 at mean percentages of 65.5%, 92.9%, 55.8%, and 84.5%, respectively (Figure 4A). Macrophages showed high expression of CD11b and CD14 at mean percentages of 94.7% and 92%, respectively (Figure 4B). The AR and ORO staining revealed the capacity of AD-MSCs in differentiation into the osteogenic lineage (calcium mineralization visualized in red color), and adipogenic lineage differentiation (lipid vacuoles visualized in red color), respectively (Figure 4C,D).

### 3.2.2 | In vitro cyto-biocompatibility assay

#### Cell viability assay

MTT assay indicated a significant increase in the proliferation and viability of the AD-MSCs grown on the DPS compared to the control group ( $p \leq 0.05$ ) (Figure 5A).

#### Cell attachment under SEM

The morphology of the DPS before and after seeding with AD-MSCs was observed under SEM (Figure 5B,C). Yellow arrows show the attached cells and grown on the DPS (Figure 5C).

#### H&E staining

The DPS samples without and with AD-MSCs were stained with H&E and viewed under the light microscope (Figure 5D,E). Yellow arrows show the cells that were grown and penetrated the pores of the DPS (Figure 5E).

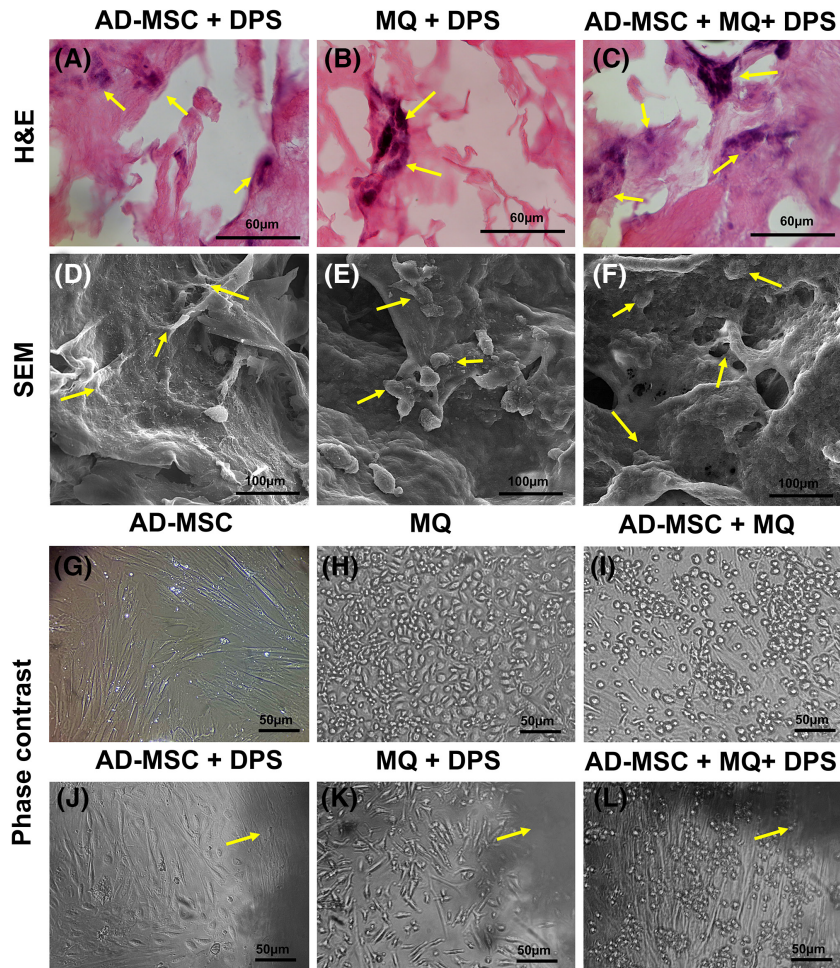


**FIGURE 6** H&E staining of the DPS (A) with AD-MSCs, (B) with macrophages (MQ), (C) with AD-MSCs + MQ. SEM micrographs of the DPS (D) with AD-MSCs, (E) with MQ, (F) with AD-MSCs + MQ. (C) the phase-contrast microscope pictures of culture groups without the DPS: (G) AD-MSCs, (H) MQ, (I) AD-MSCs + MQ. (D) the phase-contrast microscope pictures of culture groups with the DPS: (J) AD-MSCs, (K) MQ, (L) AD-MSCs + MQ. The DPS are indicated with yellow arrows.

### 3.3 | Macrophage/AD-MSCs coculture on DPS and bone lineage differentiation assays

#### H&E staining

The H&E staining images revealed the penetration and well growth of macrophage and AD-MSCs alone or coculture on DPS (Figure 6A–C).

#### SEM

The attachment and cytocompatibility of macrophages either in cocultured with AD-MSCs or alone were observed under the SEM (Figure 6D–F).

#### Phase-contrast microscopy

The morphology of macrophages, AD-MSCs, and coculture groups with or without exposure to the DPS were observed under the phase-contrast microscope after 14 days (Figure 6G–L). Macrophages cultured alone appear flattened, but the macrophages cocultured with AD-MSCs or exposed to the DPS take on more elongated shapes (Figure 6H,K). The results suggest that the morphology of macrophages that were exposed to

AD-MSCs and DPS were similar to M2 macrophages (Figure 6H–L).

#### Alizarin red staining

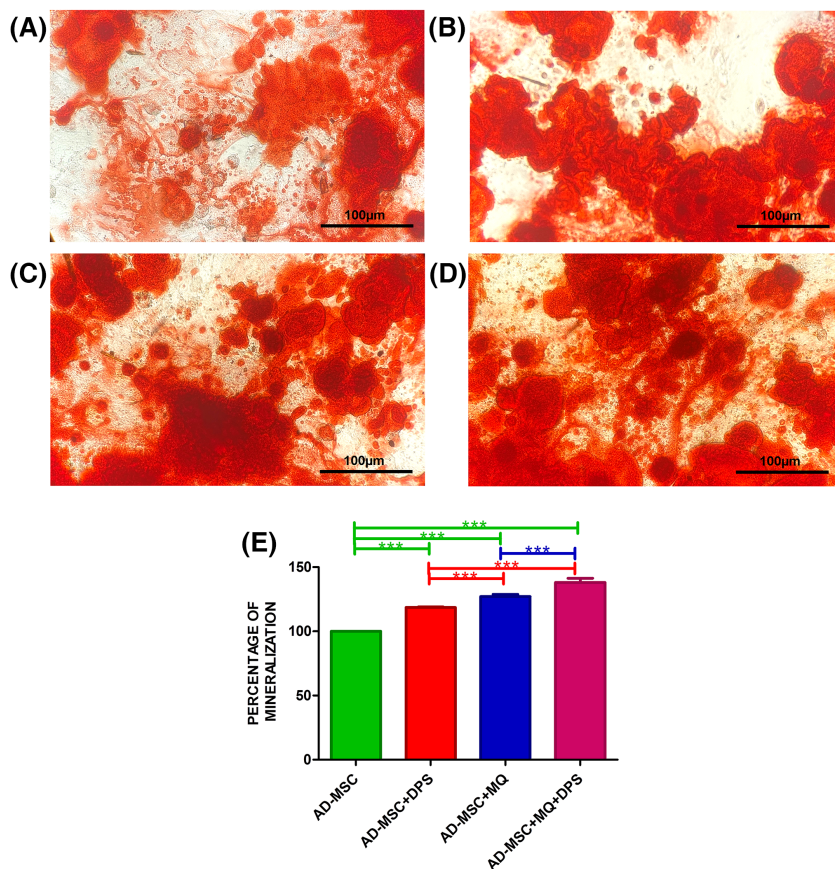
Figure 7A–D showed the induced osteogenic differentiation of the AD-MSCs alone or cocultured with macrophage on plate or DPS for 21 days. Calcium mineralization was visualized with Alizarin red staining. The ImageJ analysis revealed the highest osteogenic differentiation rate in the AD-MSCs cocultured with macrophage on DPS compared with other groups (five random fields of each group) ( $p < 0.05$ ). The AD-MSCs cultured on DPS showed an increased osteogenic differentiation compared to the same cells cultured on a cell culture plate ( $p < 0.05$ ). The AD-MSCs cocultured with macrophage on cell culture plate showed a higher level of osteogenic differentiation when compared with AD-MSCs on DPS ( $p < 0.05$ ).

#### Gene expression analyses of AD-MSCs

The relative expression of OCN, OPN, ALP, and Runx2 genes among the experimental groups are shown in Figure 8A–D. All osteogenic genes showed increased expression in cocultured groups on DPS after the induction



**FIGURE 7** Alizarin red staining after 21 days. (A) AD-MSCs, (B) AD-MSCs with the DPS, (C) AD-MSCs with macrophages (MQ), (D) AD-MSCs with the DPS and MQ, (E) percentage of mineralization were analyzed by ImageJ.



of 14 and 21 days of osteogenic differentiation. On day 14, AD-MSCs cocultured with macrophages on DPS showed the highest expression of OCN and OPN genes between the experimental groups ( $p < 0.05$ ). On day 21, the expression of OCN and OPN in both AD-MSCs cocultured with macrophages on DPS and without DPS was higher than in the other groups ( $p < 0.05$ ). The expression of ALP in AD-MSCs cocultured with macrophages on DPS was significantly increased ( $p < 0.05$ ). Runx2 in both AD-MSCs cocultured with macrophages on DPS and without DPS were considerably higher than the other groups at days 14 and 21 ( $p < 0.05$ ).

### 3.4 | In vivo biocompatibility and angiogenic property

Macroscopic observation of the implanted site revealed improved angiogenesis (black arrows) in the DPS implanted groups compared with control (no scaffold) after 7 and 28 days (Figure 9). Widespread newly-formed blood vessels (yellow arrows) in DPS implanted site were detected and confirmed by H&E staining (Figure 9). No sign of host immune response or graft rejection was observed in H&E sections of the implanted sites during 21 and 28 days of subcutaneous implantation follow-up.

## 4 | DISCUSSION

The high demand for biomaterial scaffolds for providing the naturally derived platform mimicking the structure and composition of natural bone tissue, delivering the cells to the local site of injury and facilitating the repair of bone defects has opened a window of hope in the treatment of large bone tissue fractures.<sup>34–36</sup> ECM of the placenta contains various bioactive molecules, including cytokines and growth factors such as EGF, bFGF, PDGF, IGF-1, and VEGF, suitable for bone, cartilage and blood vessel regeneration.<sup>37,38</sup> Placental tissues are readily available and with fewer ethical restrictions. This study fabricated a naturally-derived sponge by freeze-during the decellularized placental tissue. We investigated the potential of the decellularised placental sponges (DPS) as a naturally derived matrix substrate for macrophage and AD-MSCs coculture and bone lineage differentiation. Maes et al. demonstrated that the growth factors present in placental ECM are excellent for the newly formed bone.<sup>39</sup> A biological-based scaffold made from decellularized cartilage matrix (DCM) of porcine articular cartilage showed great potential for macrophage polarization to a constructive macrophage phenotype. It was indicated that the polarized macrophages promoted the BMSCs proliferation, migration,

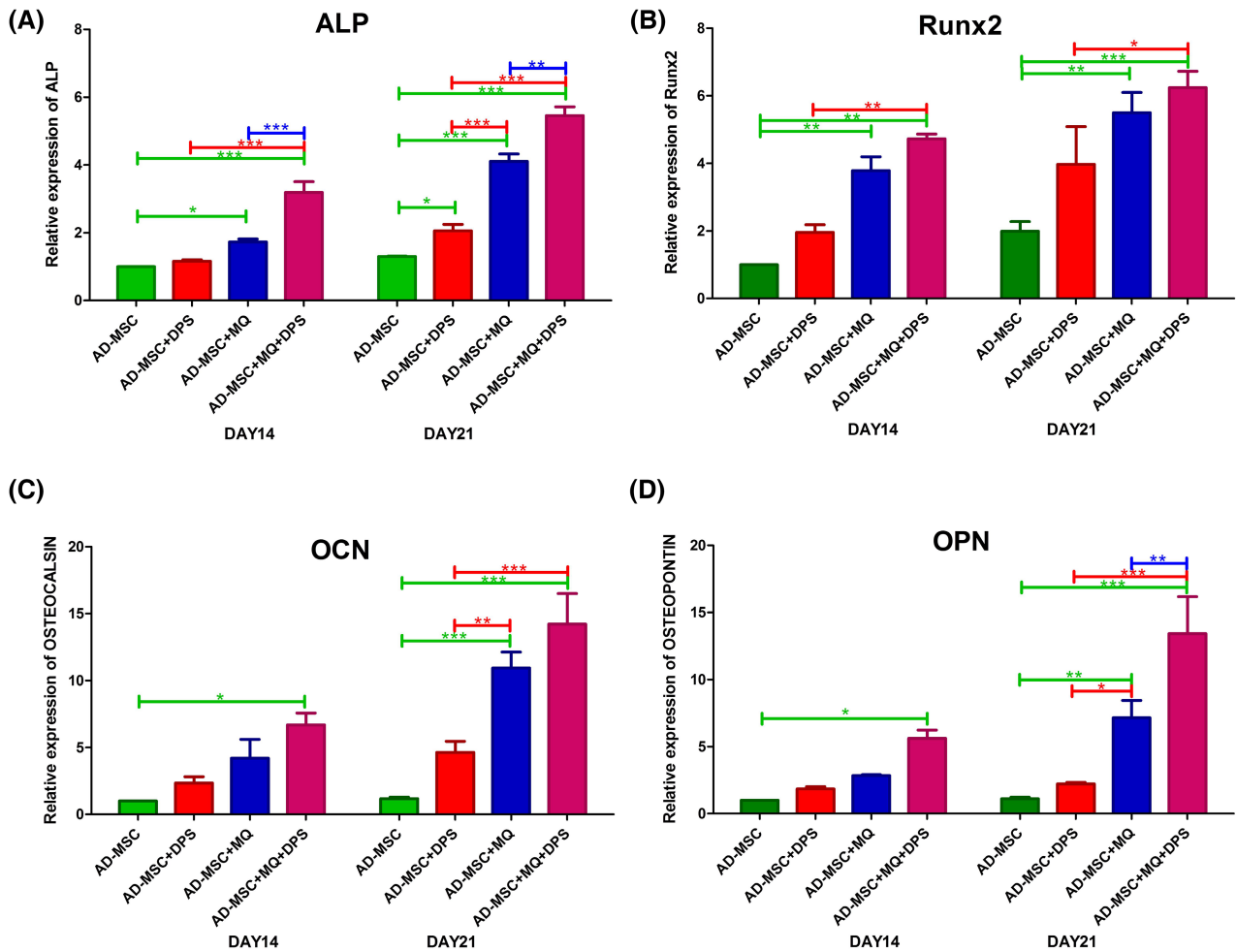


**FIGURE 8** The relative osteogenic-specific genes ([A] ALP, [B] Runx2, [C] OCN, and [D] OPN) expression analysis using RT-PCR at days 14 and 21 in AD-MSCs cultured in different coculture experimental groups.

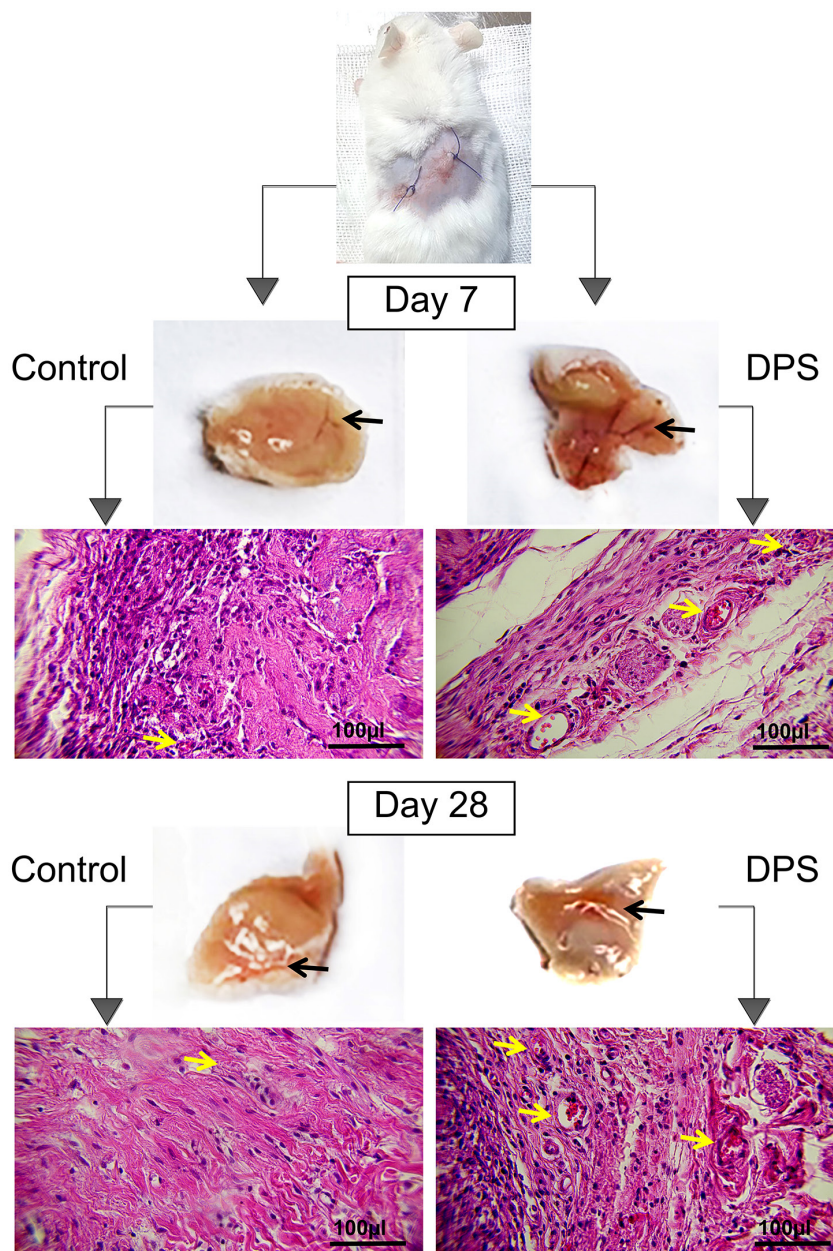
invasion, and chondrogenic differentiation in vitro.<sup>6</sup> Based on our results, the DPS had 67% porosity with an average pore size of 238 μm. Previous studies indicated that bone tissue scaffolds with large pores and high porosity could enhance bone repair after surgery. Pore sizes ranged between 100-500 μm in bone tissue scaffolds showed to be optimal for bone healing.<sup>29</sup> The in vitro degradation assay of the DPS showed around 25% weight loss during 30 days in PBS. Bone generally takes 6 to 12 weeks to heal significantly, depending on defect size and site.<sup>40,41</sup> The degradation rate of DPS is suitable for bone tissue engineering applications.

Among the cells used for cell therapy in bone defects, mesenchymal stem cells (MSCs) have many favorable characteristics, making them an excellent choice for this purpose.<sup>42</sup> In addition, because of their broad immunomodulatory properties, they are attractive targets for use in tissue engineering applications. Preosteoblasts and macrophages have physical contact in the bone niche, and their crosstalk can mediate bone formation in the sites of defects.<sup>43</sup> Still, there are many things unknown about the

interaction between MSCs and macrophages during bone regeneration. The general paradigm of macrophage functional polarization in tissue regeneration suggests that M1 macrophages contribute to the initial acute inflammatory stage and debris clearance from the fracture site.

In contrast, growth factors secreted by M2 macrophages support MSC-mediated bone formation in the later stages of fracture healing.<sup>10,44</sup> Coculture of M1 and M2 macrophages with MSCs showed that both phenotypes of macrophages influenced osteogenic differentiation differently: M1 macrophages improved the proinflammatory stage of bone repair without increasing matrix mineralization, but M2 macrophages enhanced matrix mineralization in proliferation and regeneration stage of bone healing process.<sup>45</sup> DPS-cell interaction assays revealed cytocompatibility of DPS for both AD-MSCs and macrophages in vitro. DPS induced the cells' metabolic activity and cell viability during 3 and 7 days cell culture in vitro compared with the control group. The coculture of AD-MSCs with macrophages on the DPS showed a significant upregulation of osteogenic lineage

**FIGURE 9** In vivo biocompatibility of DPS at days 7 and 28. Black and yellow arrows show newly generated vessels on samples. Control (no scaffold).



gene (OCN, OPN, ALP, and Runx2) expressions in AD-MSCs during 14 and 21 days follow-up when compared with AD-MSCs alone or cocultured with macrophage on the plastic surface of culture plate, and AD-MSCs on DPS. The upregulation of these genes may be because of the interaction between macrophages and AD-MSCs, the secretion of chemokines and cytokines like OSM, and the growth factors of DPS. The Alizarin Red staining revealed that the coculture group on the DPS had a significantly higher mineralization rate than other groups. Gong and coworkers showed that osteogenic differentiation of bone marrow mesenchymal stem cells (BMSCs) were promoted through the upregulation of ALP, Runx-2, OCN, and OPN gene expression in MQ/BMSCs coculture system treated with curcumin. Macrophage/MSCs coculture system was

suggested to promote osteoblast differentiation by increasing ALP, osteogenic markers, and bone mineralization in vitro.<sup>13</sup> Our gene expression assay and bone-specific cell staining revealed the positive effect of DPS in osteogenic cells differentiation in vitro. In vivo biocompatibility assay of subcutaneously implanted DPS demonstrated a promoted new vessel formation within the implanted site and no sign of graft rejection and host immune response.

## 5 | CONCLUSION

Our findings suggest decellularized placental sponge as an excellent bone substitute providing a naturally derived matrix with biostructure close to natural bone, a



promising coculture substrate for crosstalk of macrophage and mesenchymal stem cells in vitro, and guiding the differentiation of stem cells toward bone cells. This study offers the scientific foundations for more in vitro and in vivo investigations with the therapeutic goals of regulating the microenvironment of fracture sites for normal bone formation.

### AUTHOR CONTRIBUTION

MG and SMH conceived and designed the study. ZK, MG, and SM-Y performed the experiments. MG, SMH, MM, PBM, SCK, LM, and SM-Y analyzed the data and interpreted the results. ZK, MG, and SMH prepared the manuscript. MG, SMH, LM, SCK, MM, and SM-Y reviewed during the manuscript preparation and revised the manuscript.

### ACKNOWLEDGMENTS

This study was funded by a grant from the Iran University of Medical Sciences under grant number (16775) and Shahid Beheshti University of Medical Sciences grant number (25527). SCK has been European Research Area Chair of the FoReCaSt program of the European Commission.

### CONFLICT OF INTEREST

The authors declare that they have no known competing financial interests or personal relationships that could have influenced the work reported in this paper.

### ORCID

Seyed Mahmoud Hashemi  <https://orcid.org/0000-0003-1389-5803>

Mazaher Gholipourmalekabadi  <https://orcid.org/0000-0001-6287-6831>

### REFERENCES

- Perić Kačarević Ž, Rider P, Alkildani S, Retnasingh S, Pejakić M, Schnettler R, et al. An introduction to bone tissue engineering. *Int J Artif Organs*. 2020;43:69–86.
- Pajarinen J, Lin T, Gibon E, Kohno Y, Maruyama M, Nathan K, et al. Mesenchymal stem cell-macrophage crosstalk and bone healing. *Physiol Behav*. 2017;176:139–48.
- Kiernan C, Knuth C, Farrell E. Endochondral ossification: recapitulating bone development for bone defect repair. In: *Developmental biology and musculoskeletal tissue engineering: principles and applications*. Amsterdam: Elsevier; 2018. p. 125–48.
- Wasnik S, Rundle CH, Baylink DJ, Yazdi MS, Carreon EE, Xu Y, et al. 1,25-dihydroxyvitamin D suppresses M1 macrophages and promotes M2 differentiation at bone injury sites. *JCI Insight*. 2018;3(17):1–14.
- Uccelli A, Moretta L, Pistoia V. Mesenchymal stem cells in health and disease. *Nat Rev Immunol*. 2008;8:726–36.
- Tian G, Jiang S, Li J, Wei F, Li X, Ding Y, et al. Cell-free decellularized cartilage extracellular matrix scaffolds combined with interleukin 4 promote osteochondral repair through immunomodulatory macrophages: in vitro and in vivo preclinical study. *Acta Biomater*. 2021;127:131–45.
- Wu AC, Raggatt LJ, Alexander KA, Pettit AR. Unraveling macrophage contributions to bone repair. *Bonekey Rep*. 2013;2:1–7.
- Chang MK, Raggatt L-J, Alexander KA, Kuliwaba JS, Fazzalari NL, Schroder K, et al. Osteal tissue macrophages are intercalated throughout human and mouse bone lining tissues and regulate osteoblast function in vitro and in vivo. *J Immunol*. 2008;181(2):1232–44.
- Alexander KA, Chang MK, Maylin ER, Kohler T, Müller R, Wu AC, et al. Osteal macrophages promote in vivo intramembranous bone healing in a mouse tibial injury model. *J Bone Miner Res*. 2011;26(7):1517–32.
- Niu Y, Wang Z, Shi Y, Dong L, Wang C. Modulating macrophage activities to promote endogenous bone regeneration: biological mechanisms and engineering approaches. *Bioact Mater*. 2021;6:244–61.
- Hozain S, Cottrell J. CD11b+ targeted depletion of macrophages negatively affects bone fracture healing. *Bone*. 2020;138:115479.
- Murray PJ. Macrophage polarization. *Annu Rev Physiol*. 2017;79(10):541–66.
- Gong L, Zhao Y, Zhang Y, Ruan Z. The macrophage polarization regulates MSC osteoblast differentiation in vitro. *Ann Clin Lab Sci*. 2016;46(1):65–71.
- Guihard P, Boutet MA, Brounais-Le Royer B, Gamblin AL, Amiaud J, Renaud A, et al. Oncostatin M, an inflammatory cytokine produced by macrophages, supports intramembranous bone healing in a mouse model of tibia injury. *Am J Pathol*. 2015;185(3):765–75.
- Vi L, Baht GS, Whetstone H, Ng A, Wei Q, Poon R, et al. Macrophages promote osteoblastic differentiation in-vivo: implications in fracture repair and bone homeostasis. *J Bone Miner Res*. 2015;30(6):1090–102.
- Maggini J, Mirkin G, Bognanni I, Holmberg J, Piazzón IM, Nepomnaschy I, et al. Mouse bone marrow-derived mesenchymal stromal cells turn activated macrophages into a regulatory-like profile. *PLoS One*. 2010;5(2):9252.
- Kim J, Hematti P. Mesenchymal stem cell-educated macrophages: a novel type of alternatively activated macrophages. *Exp Hematol*. 2009;37(12):1445–53.
- Re F, Gabusi E, Manferdini C, Russo D, Lisignoli G. Bone regeneration improves with mesenchymal stem cell derived extracellular vesicles (EVs) combined with scaffolds: a systematic review. *Biology*. 2021;10(7):579.
- Zeng JH, Qiu P, Xiong L, Liu SW, Ding LH, Xiong SL, et al. Bone repair scaffold coated with bone morphogenetic protein-2 for bone regeneration in murine calvarial defect model: systematic review and quality evaluation. *Int J Artif Organs*. 2019;42:325–37.
- Jin J, Wang J, Huang J, Huang F, Fu J, Yang X, et al. Transplantation of human placenta-derived mesenchymal stem cells in a silk fibroin/hydroxyapatite scaffold improves bone repair in rabbits. *J Biosci Bioeng [Internet]*. 2014;118(5):593–8. <https://doi.org/10.1016/j.jbiosc.2014.05.001>
- Rameshbabu AP, Ghosh P, Subramani E, Bankoti K, Kapat K, Datta S, et al. Investigating the potential of human placenta-derived extracellular matrix sponges coupled with amniotic membrane-derived stem cells for osteochondral tissue engineering. *J Mater Chem B*. 2016;4(4):613–25.



22. Gholipourmalekabadi M, Farhadhosseinabadi B, Faraji M, Nourani MR. How preparation and preservation procedures affect the properties of amniotic membrane? How safe are the procedures? *Burns*. 2020;46:1254–71.
23. Zhang X, Wang N, Huang Y, Li Y, Li G, Lin Y, et al. Extracellular vesicles from three dimensional culture of human placental mesenchymal stem cells ameliorated renal ischemia/reperfusion injury. *Int J Artif Organs*. 2022;45(2):181–92.
24. Komemi O, Shochet GE, Pomeranz M, Fishman A, Pasmanik-Chor M, Drucker L, et al. Placenta-fv (ECM) activates breast cancer cell survival mechanisms: a key for future distant metastases *Int J Cancer*. 2018;144(7):1633–44.
25. Carvalho CMF, Leonel LCPC, Cañada RR, Barreto RSN, Maria DA, Del Sol M, et al. Comparison between placental and skeletal muscle ECM: in vivo implantation. *Connect Tissue Res*. 2021;62(6):629–42.
26. Lee JS, Romero R, Han YM, Kim HC, Kim CJ, Hong JS, et al. Placenta-on-a-chip: a novel platform to study the biology of the human placenta. *J Matern Neonatal Med*. 2016;29(7):1046–54.
27. Asgari F, Khosravimelal S, Koruji M, Aliakbar Ahovan Z, Shirani A, Hashemi A, et al. Long-term preservation effects on biological properties of acellular placental sponge patches. *Mater Sci Eng C [Internet]*. 2021;121(September 2020):111814. <https://doi.org/10.1016/j.msec.2020.111814>
28. Asgari F, Asgari HR, Najafi M, Eftekhari BS, Vardiani M, Gholipourmalekabadi M, et al. Optimization of decellularized human placental macroporous scaffolds for spermatogonial stem cells homing. *J Mater Sci Mater Med*. 2021;32(5):47.
29. Karageorgiou V, Kaplan D. Porosity of 3D biomaterial scaffolds and osteogenesis. *Biomaterials*. 2005;26(27):5474–91.
30. Khosrowpour Z, Hashemi SM, Mohammadi-Yeganeh S, Soudi S. Pretreatment of mesenchymal stem cells with leishmania major soluble antigens induce anti-inflammatory properties in mouse peritoneal macrophages. *J Cell Biochem*. 2017;118(9):2764–79.
31. Mokhtari S, Solati-Hashjin M, Khosrowpour Z, Gholipourmalekabadi M. Layered double hydroxide-galactose as an excellent nanocarrier for targeted delivery of curcumin to hepatocellular carcinoma cells. *Appl Clay Sci*. 2020;200:105891.
32. Simorgh S, Alizadeh R, Eftekhazadeh M, Haramshahi SMA, Milan PB, Doshmanziari M, et al. Olfactory mucosa stem cells: an available candidate for the treatment of the Parkinson's disease. *J Cell Physiol*. 2019;234(12):23763–73.
33. Yazdanpanah A, Majidi Z, Pezeshki-Modaress M, Khosrowpour Z, Farshi P, Eini L, et al. Bioengineering of fibroblast-conditioned polycaprolactone/gelatin electrospun scaffold for skin tissue engineering. *Artif Organs*. 2022;46(6):1040–54.
34. Akdere ÖE, Shikhaliyeva İ, Gümüşderelioğlu M. Boron mediated 2D and 3D cultures of adipose derived mesenchymal stem cells. *Cytotechnology*. 2019;71(2):611–22.
35. Zhang Y, Wu D, Zhao X, Pakvasa M, Tucker AB, Luo H, et al. Stem cell-friendly scaffold biomaterials: applications for bone tissue engineering and regenerative medicine. *Front Bioeng Biotechnol*. 2020;8:598607.
36. Farhadhosseinabadi B, Zarebkohan A, Eftekhary M, Heiat M, Moosazadeh Moghaddam M, Gholipourmalekabadi M. Crosstalk between chitosan and cell signaling pathways. *Cell Mol Life Sci*. 2019;76(14):2697–718.
37. Werner S, Grose R. Regulation of wound healing by growth factors and cytokines. *Physiol Rev*. 2003;83(3):835–70.
38. Özdemir E, Emet A, Hashemihesar R, Yürüker ACS, Kılıç E, Uçkan Çetinkaya D, et al. Articular cartilage regeneration utilizing decellularized human placental scaffold, mesenchymal stem cells and platelet rich plasma. *Tissue Eng Regen Med*. 2020;17(6):901–8.
39. Maes C, Coenegrachts L, Stockmans I, Daci E, Luttun A, Petryk A, et al. Placental growth factor mediates mesenchymal cell development, cartilage turnover, and bone remodeling during fracture repair. *J Clin Invest*. 2006;116(5):1230–42.
40. O'Keefe RJ. Fibrinolysis as a target to enhance fracture healing. *N Engl J Med*. 2015;373(18):1776–8.
41. Wong RMY, Choy VMH, Li J, Li TK, Chim YN, Li MCM, et al. Fibrinolysis as a target to enhance osteoporotic fracture healing by vibration therapy in a metaphyseal fracture model. *Bone Jt Res*. 2021;10(1):41–50.
42. Lin W, Xu L, Zwingenberger S, Gibon E, Goodman SB, Li G. ScienceDirect mesenchymal stem cells homing to improve bone healing. *J Orthop Transl [Internet]*. 2017;9:19–27. <https://doi.org/10.1016/j.jot.2017.03.002>
43. Loi F, Córdova LA, Zhang R, Pajarinen J, Lin TH, Goodman SB, et al. The effects of immunomodulation by macrophage subsets on osteogenesis in vitro. *Stem Cell Res Ther*. 2016;7(1):15.
44. Zhang R, Liang Y, Wei S. M2 macrophages are closely associated with accelerated clavicle fracture healing in patients with traumatic brain injury: a retrospective cohort study. *J Orthop Surg Res*. 2022;13(1):213.
45. Zhang Y, Böse T, Unger RE, Jansen JA, Kirkpatrick CJ, Van Den Beucken JJJP. Macrophage type modulates osteogenic differentiation of adipose tissue MSCs. *Cell Tissue Res*. 2017;369(2):273–86.

**How to cite this article:** Khosrowpour Z, Hashemi SM, Mohammadi-Yeganeh S, Moghtadaei M, Brouki Milan P, Moroni L, et al. Coculture of adipose-derived mesenchymal stem cells/macrophages on decellularized placental sponge promotes differentiation into the osteogenic lineage. *Artif. Organs*. 2022;00:1–15. <https://doi.org/10.1111/aor.14394>